

# UC Davis

## UC Davis Previously Published Works

### Title

Efficient Approach for the Reliability-Based Design of Linear Damping Devices for Seismic Protection of Buildings

### Permalink

<https://escholarship.org/uc/item/96j0q6mq>

### Journal

ASCE-ASME Journal of Risk and Uncertainty in Engineering Systems Part A Civil Engineering, 2(2)

### ISSN

2376-7642

### Authors

Tubaldi, E  
Barbato, M  
Dall'Asta, A

### Publication Date

2016-06-01

### DOI

10.1061/ajrua6.0000858

Peer reviewed

# Efficient approach for the reliability- based design of linear damping devices for seismic protection of buildings

E. Tubaldi<sup>1</sup>, M. Barbato, M.ASCE<sup>2</sup>, A. Dall'Asta<sup>3</sup>

<sup>1</sup>Postdoctoral Researcher, School of Architecture and Design, University of Camerino, Viale della Rimembranza, 63100 Ascoli Piceno (AP), Italy; E-mail: [etubaldi@gmail.com](mailto:etubaldi@gmail.com)

<sup>2</sup>Associate Professor, Department of Civil & Environmental Engineering, Louisiana State University and A&M College, 3418H Patrick F. Taylor Hall, Nicholson Extension, Baton Rouge, Louisiana 70803, USA; E-mail: [mbarbato@lsu.edu](mailto:mbarbato@lsu.edu) (corresponding author)

<sup>3</sup>Professor, School of Architecture and Design, University of Camerino, Viale della Rimembranza, 63100 Ascoli Piceno (AP), Italy; E-mail: [a.asta@tin.it](mailto:a.asta@tin.it)

## Abstract

This paper presents an efficient reliability-based methodology for the seismic design of viscous/visco-elastic dissipative devices in independent and/or coupled buildings. The proposed methodology is consistent with modern performance-based earthquake engineering frameworks and explicitly considers the uncertainties affecting the seismic input and the model parameters, as well as the correlation between multiple limit states.

The proposed methodology casts the problem of the dampers' design for a target performance objective in the form of a reliability-based optimization problem with a probabilistic constraint. The general approach proposed in this study is specialized to stochastic seismic excitations and performance levels for which the structural behavior can be assumed linear elastic. Under these conditions, the optimization problem is solved efficiently by taking advantage of existing analytical techniques for estimating the system reliability. This analytical design solution is an approximation of the optimal design and can be used as a hot-start point for simulation-based techniques, which can be employed to find the optimal design solution. An efficient correction formula is proposed to obtain an improved design solution that is generally sufficiently close for engineering purposes to the optimal design solution obtained from significantly more computationally expensive simulation-based techniques. The proposed design methodology is illustrated and validated by considering two steel buildings modeled as linear elastic multi-degree-of-freedom systems

29 for different linear damper properties and collocation, for both independent and coupled configurations.

30 KEY WORDS: performance-based earthquake engineering; linear viscous dampers; visco-elastic dampers; design  
31 procedure; non-stationary random process; reliability-based optimization.

## 32 **Introduction**

33 The use of supplemental damping in the form of viscous or visco-elastic dampers has become increasingly  
34 widespread in the design and retrofit of civil structures excited by earthquake loads because it often permits  
35 to mitigate undesirable aspects of the structural response at a lower cost than other more traditional  
36 approaches. Experimental and analytical studies have demonstrated that the addition of viscous or visco-  
37 elastic dampers inside a building (Soong and Spencer 2002, Takewaki 2009) and/or between adjacent  
38 buildings (Zhang and Xu 1999, Kim et al. 2006, Roh et al. 2011, Tubaldi 2015) permits to control motion  
39 amplitude, interstory drifts, and absolute accelerations induced by earthquake actions.

40 In recent years, different methodologies for the optimal design of these damping devices under uncertain  
41 seismic input were proposed. However, significant simplifications were often introduced to reduce the  
42 complexity of the problem. Several of the design methods proposed in the literature (Shukla and Datta  
43 1999, Takewaki 2009, Zhu et al. 2011, Richardson et al. 2012) expressed the performance objectives in  
44 terms of mean-square displacement or interstory drift response of the buildings, without explicit reliability  
45 considerations in terms of damage and loss risk. Numerous studies employed simple stochastic models  
46 (e.g., stationary white noise or Kanai-Tajimi models) to describe the seismic input, by disregarding its non-  
47 stationary characteristics (e.g., Bhaskararao and Jangid 2007, Takewaki 2009, Taflanidis and Scruggs 2010,  
48 Taflanidis 2010, Zhu et al. 2011). Only a few studies considered explicitly the effects of (1) model  
49 parameter uncertainty (MPU) (i.e., the uncertainty affecting the parameters used to define both the structural  
50 model and/or the limit states), which can have a non-negligible influence on the structural performance  
51 (Guo et al. 2002, Taflanidis 2010); and (2) correlation between different component response and failure  
52 modes in evaluating the system reliability (Taflanidis 2010, Taflanidis and Scruggs 2010). The latter effects  
53 may significantly influence the seismic reliability estimates for a given system, especially in the case of  
54 adjacent buildings connected by dampers (Tubaldi et al. 2014).

55 In the last decade, significant progress was made towards overcoming the aforementioned limitations in

56 reliability-based design procedures for passively-damped buildings. Marano et al. (2007) developed a  
57 reliability-based design approach for linear multi-story frames protected by using linear viscous dampers.  
58 This approach was based on the minimization of a deterministic objective function defined as the total  
59 added damping, while stochastic constraints were imposed to limit the system failure probability for a given  
60 earthquake hazard level. Taflanidis (2010) presented a reliability-based methodology for the optimal design  
61 of systems subjected to stationary stochastic loading with uncertain model parameters. The study  
62 highlighted the importance of the correlation between the failure modes and MPU from a design  
63 perspective. Jensen and Sepulveda (2012) proposed a method for the design of structures equipped with  
64 passive dissipation systems by considering both record-to-record variability and MPU. The damper design  
65 was formulated as an optimization problem with a single objective function and multiple reliability  
66 constraints. The problem solution was sought through a sequential optimization approach (Jensen and  
67 Sepulveda 2011) that involved a converging series of approximate reliability analyses.

68 The present study presents a simple yet comprehensive probabilistic methodology for the reliability-based  
69 design of viscous/visco-elastic dampers that are added to structural systems subject to seismic hazard. This  
70 methodology explicitly considers the uncertainties affecting the seismic input and the model parameters, as  
71 well as the correlation between multiple limit states. The problem of the design for a target performance  
72 objective is cast in the form of a reliability-based optimization problem. Although the proposed  
73 methodology is general, in this paper it is specialized to the case of seismic excitation modeled as non-  
74 stationary stochastic processes, and performance objectives for which the structural behavior can be  
75 assumed linear elastic. This specialization permits to take advantage of recently derived time-variant  
76 reliability analysis techniques (Barbato and Conte 2008, Barbato and Vasta 2010, Barbato and Conte 2011,  
77 2014) for evaluating the system risk of deterministic systems, and to obtain an approximate optimal design  
78 at a computational cost that is several orders of magnitude lower than that required to obtain the optimal  
79 design by using simulation-based techniques. A correction formula is also proposed to derive an improved  
80 design solution at a very low computational cost. The proposed design methodology is illustrated and  
81 validated by considering two steel buildings modeled as linear elastic multi-degree-of-freedom systems

82 under different configurations and design conditions.

### 83 **Problem formulation**

#### 84 *Failure probability estimate for systems equipped with damping devices*

85 The basis of the proposed design method is the efficient solution of the direct reliability problem, which  
86 corresponds to evaluating the failure probability,  $P_{f,t_L}$ , of the system with added dampers during its design  
87 life,  $t_L$ , i.e., the probability of not satisfying the performance objective during  $t_L$ . In this type of problem,  
88 the building and dampers' properties, the seismic input characteristics, and the seismic hazard at the site  
89 are known quantities.

90 Under the assumption that the failure events can be described as a Poisson process and that the buildings  
91 are immediately restored to their original condition after failure,  $P_{f,t_L}$  is obtained as:

$$92 \quad P_{f,t_L} = 1 - e^{-v_f \cdot t_L} \quad (1)$$

93 in which  $v_f$  = mean annual frequency (MAF) of system failure, which can be computed through the  
94 following convolution integral:

$$95 \quad v_f = \int_{im} P_{f|IM}(im) \cdot |dv_{IM}(im)| \quad (2)$$

96 where  $P_{f|IM}(im)$  = fragility function expressing the probability of system failure conditional to the seismic  
97 intensity measure  $IM = im$ , and  $v_{IM}(im)$  = MAF of exceedance of a specific value  $im$  of  $IM$ . For the sake  
98 of simplicity, this study considers only scalar seismic intensity measures. The most challenging task of this  
99 direct reliability problem is the computation of the conditional failure probability,  $P_{f|IM}(im)$ . The  
100 reliability of multi-component structural systems, such as those considered in this study, depends on the  
101 reliability of its components, i.e., the building structural elements and the dampers. The computation of the  
102 conditional failure probability of the components,  $P_{f_i|IM}(im)$  ( $i = 1, 2, \dots, N_{ls}$ , where  $N_{ls}$  = number of  
103 component limit states), and of the system,  $P_{f|IM}(im)$ , requires solving a time-variant reliability problem

104 by accounting for all pertinent sources of uncertainty. The simplest approach for solving this time-variant  
 105 reliability problem is Monte Carlo simulation (MCS). However, this approach can be computationally  
 106 expensive, since it requires a very (sometimes prohibitively) large number of time-history analyses to obtain  
 107 accurate results when small failure probabilities need to be estimated. Thus, advanced simulation techniques  
 108 (Au and Beck 2001a, 2001b) or analytical techniques based on random vibration theory (Guo et al. 2002,  
 109 Park et al. 2004, Marano et al. 2007, Taflanidis 2010, Tubaldi et al. 2014) are usually preferred to MCS for  
 110 practical structural engineering applications.

### 111 *Reliability-based design of damping devices*

112 The design of the damping devices that are needed to achieve a target system failure probability over its  
 113 design life can be cast as an optimization problem, which identifies the optimal dampers properties (e.g.,  
 114 the properties that minimize a specified objective function) that also satisfy the stochastic constraints on  
 115 the probability of exceeding a prescribed damage level. Additional constraints are needed to ensure that the  
 116 dampers' properties assume physically admissible values. The objective function depends on the type of  
 117 device considered. For example, if a visco-elastic material such as rubber is employed, the dampers' cost  
 118 can be assumed proportional to the rubber volume, which can be expressed as a function of the dampers'  
 119 stiffness and geometric parameters (Park et al. 2004); whereas, for linear viscous dampers (e.g., fluid  
 120 dampers), the sum of the dampers' viscous constants can be employed as a simplified approximation for  
 121 the dampers' cost (Takewaki 2009). A more accurate cost estimate could also consider the dampers' peak  
 122 force and stroke (Hwang et al. 2013). However, the introduction of these variables would require a  
 123 stochastic objective function, whose treatment is considered out of the scope of this paper. In this study, the  
 124 design problem is mathematically formalized as follows:

$$\begin{aligned}
 & \min_{\mathbf{d}} \quad C(\mathbf{d}) \\
 & \text{subject to} \quad \mathbf{f}(\mathbf{d}) \leq 0 \\
 & \quad \quad \quad P_{f,t_L}(\mathbf{d}) - \bar{P}_f \leq 0
 \end{aligned} \tag{3}$$

126 where  $\mathbf{d} = [k_{d,1}, \dots, k_{d,m}, c_{d,1}, \dots, c_{d,m}, a_{d,1}, \dots, a_{d,m}]^T$  = vector of design variables;  $k_{d,i}$ ,  $c_{d,i}$  and  $a_{d,i}$

127  $(i = 1, 2, \dots, m)$  = stiffness, damping constant, and parameter describing the geometry, respectively, of the  
128  $i$ -th damper; the superscript  $T$  denotes matrix/vector transposition;  $m$  = total number of dampers;  $\mathbf{f}(\mathbf{d}) \leq 0$   
129 = additional (linear and/or nonlinear) deterministic constraints specifying the feasible domain of the damper  
130 properties;  $C(\mathbf{d})$  = deterministic objective function; and  $\bar{P}_f$  = target (design) failure probability.  
131 The evaluation of  $P_{f,t_L}(\mathbf{d})$  (in which the explicit dependency on the design variables  $\mathbf{d}$  is shown for  
132 clarity) is the most computationally challenging task in the design procedure corresponding to Eq. (3). This  
133 study focuses on the development of efficient solution techniques based on the assumption of linear elastic  
134 structural behavior. In fact, the dampers are often employed to achieve performance levels corresponding  
135 to negligible structural damage, e.g., immediate occupancy or operational performance level, as defined in  
136 FEMA 273 (1997) and FEMA 356 (2000). For these performance levels, the assumption of linear elastic  
137 structural behavior is satisfied.

### 138 **Efficient solution of the reliability-based design of structural systems with added dampers**

139 This section describes an efficient methodology for solving the reliability-based design problem defined by  
140 Eqs. (1) through (3) for performance levels corresponding to linear elastic behavior of the structural systems  
141 under consideration. First, the equations of motion of a general system of two building coupled using  
142 viscous/visco-elastic dampers and the seismic input model are introduced. Then, an efficient methodology  
143 for obtaining an approximate solution for the design problem expressed by Eq. (3) is presented. Finally, a  
144 correction formula to improve the approximate optimal design at a very low computational cost is proposed.

#### 145 *Equations of motion for coupled buildings with added dampers*

146 Under the assumption of linear elastic behavior, the equations of motion of two adjacent buildings with  
147 dampers added both inside and between the building's frames (Fig. 1) can be written as follows:

$$148 \quad \mathbf{M} \cdot \ddot{\mathbf{U}}(t) + (\mathbf{C} + \mathbf{C}_d) \cdot \dot{\mathbf{U}}(t) + (\mathbf{K} + \mathbf{K}_d) \cdot \mathbf{U}(t) = -\mathbf{M} \cdot \mathbf{R} \cdot \ddot{\mathbf{U}}_g(t) \quad (4)$$

149 in which  $\mathbf{U} = \begin{bmatrix} \mathbf{U}_A \\ \mathbf{U}_B \end{bmatrix}$ ;  $\mathbf{M} = \begin{bmatrix} \mathbf{M}_A & \mathbf{0} \\ \mathbf{0} & \mathbf{M}_B \end{bmatrix}$ ;  $\mathbf{K} = \begin{bmatrix} \mathbf{K}_A & \mathbf{0} \\ \mathbf{0} & \mathbf{K}_B \end{bmatrix}$ ;  $\mathbf{C} = \begin{bmatrix} \mathbf{C}_A & \mathbf{0} \\ \mathbf{0} & \mathbf{C}_B \end{bmatrix}$ ;  $\mathbf{U}_i$  = displacement vector

150 of the free degrees-of-freedom of building  $i$  ( $i = A, B$ );  $\mathbf{M}_i, \mathbf{K}_i,$  and  $\mathbf{C}_i$  = mass, stiffness, and damping  
151 matrices of building  $i$  ( $i = A, B$ ), respectively;  $\mathbf{K}_d$  and  $\mathbf{C}_d$  = stiffness and damping matrices corresponding  
152 to the added dampers, respectively;  $\mathbf{R}$  = influence coefficient matrix;  $\ddot{\mathbf{U}}_g(t)$  = vector containing the  
153 different components of the input ground motion;  $t$  = time; and a superposed dot denotes differentiation  
154 with respect to time. The equations of motion of a single building with added dampers are a particular sub-  
155 case of Eq. (4).

156 Matrices  $\mathbf{K}_d$  and  $\mathbf{C}_d$  contain the information regarding both the properties and the location of the dampers  
157 within and/or between the buildings (see Fig. 1). Any set of structural responses that can be obtained from  
158 the displacement response vector  $\mathbf{U}(t)$  by means of a linear operator (e.g., interstory drifts, base shear,  
159 floor shears) can be used as engineering demand parameter to monitor the response of the system  
160 components.

161 In this paper, the input ground acceleration components are modeled as separable non-stationary stochastic  
162 processes (Barbato and Vasta 2010). This analytical representation of the seismic input is completely  
163 defined by a power spectral density (PSD) function of an embedded Gaussian stationary process and by a  
164 deterministic time-modulating function. The parameters needed to describe both the PSD and the time-  
165 modulating functions must be appropriately chosen in order to accurately represent the characteristics of  
166 the seismic input expected at the site (e.g., frequency content, spectral acceleration at specified frequencies,  
167 and input duration). The description of the seismic input is completed by an appropriate hazard function for  
168 the site, i.e.,  $v_{IM}(im)$ . The  $IM$  should be selected based on sufficiency and efficiency criteria (Luco and  
169 Cornell 2007) and should be easily related to the stochastic description of the input ground motion process.  
170 It is noteworthy that, if multiple active seismic sources can affect the site of interest, a different seismic  
171 ground motion model can be used for each source.

## 172 ***Efficient approximate solution of the reliability-based design problem***

173 A previous study by the authors (Tubaldi et al. 2014) proposed an analytical technique for the seismic risk



174 assessment of adjacent buildings connected by linear and nonlinear viscous/visco-elastic dampers. In  
 175 particular, the seismic risk  $P_{f,t_L}$  for deterministic systems can be efficiently and accurately approximated  
 176 by (1) evaluating the component fragilities  $P_{f_i|IM}(im)$  ( $i=1,2,\dots,N_{ls}$ , where  $N_{ls}$  = number of  
 177 component limit states) by solving a first-passage reliability problem through the use of approximate  
 178 analytical time-variant hazard functions (i.e., based on the Poisson's, classical Vanmarcke's, or modified  
 179 Vanmarcke's approximations); (2) estimating the system failure probability conditional to  $im$ ,  $P_{f|IM}(im)$ ,  
 180 by using a series system idealization and assuming perfectly correlated limit states; and (3) computing the  
 181 MAF of the system failure,  $v_f$ , and the failure probability over the design life of the structural system,  
 182  $P_{f,t_L}$ , via Eqs. (2) and (1), respectively. In the case of systems with uncertain properties, the computation  
 183 of  $P_{f_i|IM}(im)$  ( $i=1,2,\dots,N_{ls}$ ) is performed by using the total probability theorem in conjunction with  
 184 simulation techniques such as Latin hypercube sampling (LHS), as described in Tubaldi et al. (2014).  
 185 The optimization problem defined by Eq. (3) can have multiple local minima and, thus, must be solved  
 186 using global optimization techniques. In this study, a multiple start point algorithm based on gradient-based  
 187 iterative local optimizers was employed (Ugray et al. 2007, MathWorks 2015). Local optimization  
 188 algorithms require to compute repeatedly the system failure probability,  $P_{f,t_L}(\mathbf{d})$ , and its gradient with  
 189 respect to the design variables  $\mathbf{d}$ ,  $\nabla_{\mathbf{d}} P_{f,t_L}(\mathbf{d})$ . The analytical technique proposed in Tubaldi et al. (2014),  
 190 referred to as analytical (AN) algorithm, provides a smooth representation of these quantities, denoted  
 191 respectively as  $P_{f,t_L}^{AN}(\mathbf{d})$  and  $\nabla_{\mathbf{d}} P_{f,t_L}^{AN}(\mathbf{d})$ , and can be efficiently used to calculate them. The AN  
 192 algorithm neglects the effects of MPU and provides a fully analytical and computationally efficient  
 193 approximation of the reliability-based design problem. The assumption of deterministic system and the use  
 194 of analytical estimates of the first-passage failure probability in the AN algorithm also permits to avoid  
 195 numerical issues which may arise when stochastic simulation is used in conjunction with gradient-based  
 196 optimization algorithms (Taflanidis and Beck 2008, Jensen et al. 2009). The local optimization algorithm

197 is assumed to converge at iteration  $i+1$  to the solution  $\mathbf{d}_{AN,j}^*$  ( $j=1,2,\dots,n_{sp}$ , where  $n_{sp}$  = number of start  
198 points) when  $\frac{|C(\mathbf{d}_{i+1})-C(\mathbf{d}_i)|}{C(\mathbf{d}_i)} < \varepsilon_1$  and  $|P_{f,t_L}^{AN}(\mathbf{d}_{i+1})-\bar{P}_f| < \varepsilon_2$  respectively, where  $\varepsilon_1, \varepsilon_2$  = user-  
199 defined tolerances. The design solution is given by  $\mathbf{d}_{AN}^* = \min_j(\mathbf{d}_{AN,j}^*)$ .

200 In general, due to the approximate nature of the time-variant hazard function, the assumptions made on the  
201 correlation among the failure modes, and the effects of MPU that are neglected by the AN algorithm, the  
202 stochastic constraint on the system failure probability in Eq. (3) may not be strictly satisfied by the  
203 approximate design solution  $\mathbf{d}_{AN}^*$ , i.e., the condition  $|P_{f,t_L}^{SIM}(\mathbf{d}_{AN}^*)-\bar{P}_f| > \varepsilon_2$  may occur, where  
204  $P_{f,t_L}^{SIM}(\mathbf{d}_{AN}^*)$  = system failure probability evaluated through MCS at  $\mathbf{d}_{AN}^*$ . However,  $\mathbf{d}_{AN}^*$  can be used as  
205 a “hot-start” point for optimization algorithms based on stochastic simulation techniques, such as the  
206 simulation (SIM) algorithm and the hybrid (HYB) algorithms proposed in Barbato and Tubaldi (2013),  
207 whose solutions ( $\mathbf{d}_{SIM}^*$  and  $\mathbf{d}_{HYB}^*$ , respectively) strictly satisfy the constraint on the system failure  
208 probability within a user-defined tolerance. The SIM algorithm is an iterative optimization algorithm that  
209 uses the estimate of the failure probability and its gradient obtained through stochastic simulation,  
210 respectively denoted to as  $P_{f,t_L}^{SIM}(\mathbf{d})$  and  $\nabla_{\mathbf{d}}P_{f,t_L}^{SIM}(\mathbf{d})$ , whereas the HYB algorithm uses the estimate of  
211 the failure probability obtained through simulation,  $P_{f,t_L}^{SIM}(\mathbf{d})$ , in conjunction with the analytical estimate  
212 of the failure probability gradient,  $\nabla_{\mathbf{d}}P_{f,t_L}^{AN}(\mathbf{d})$ . It is noteworthy that the computational cost of the SIM  
213 and HYB algorithms is several orders of magnitude higher than the computational cost of the AN algorithm.  
214 Furthermore, numerical problems often arise when stochastic simulation is used in conjunction with  
215 gradient-based algorithms (Taflanidis and Beck 2008, Jensen et al. 2009), which may further increase the  
216 number of iterations required to achieve convergence.

217 ***Design correction formula***

218 In order to improve the approximate design solution obtained using the AN algorithm while avoiding the

219 higher computational cost of the SIM and HYB algorithms, the following correction formula for the  
 220 solution  $\mathbf{d}_{AN}^*$  is proposed in this study:

$$221 \quad \mathbf{d}_{\text{corr}}^* = \left( 1 + \frac{\bar{P}_f - P_{f,t_L}^{\text{SIM}}(\mathbf{d}_{AN}^*)}{\nabla_{\mathbf{d}} P_{f,t_L}^{\text{AN}}(\mathbf{d}_{AN}^*) \cdot \mathbf{d}_{AN}^*} \right) \cdot \mathbf{d}_{AN}^* \quad (5)$$

222 The corrected approximate design point  $\mathbf{d}_{\text{corr}}^*$  is obtained by equating to  $\bar{P}_f$  the first-order Taylor's series  
 223 approximation of the failure probability about  $\mathbf{d}_{AN}^*$  along the direction defined by  $\mathbf{d}_{AN}^*$ , with the gradient  
 224  $\nabla_{\mathbf{d}} P_{f,t_L}^{\text{AN}}(\mathbf{d}_{AN}^*)$  computed using the analytical approximation of the hazard function. Thus, the proposed  
 225 correction formula corresponds to scaling the optimal damper properties found using the AN algorithm.  
 226 Fig. 2 provides a graphical representation of the correction for a case involving two design variables. The  
 227 proposed correction formula is based on two main assumptions: (1) the design solution obtained through  
 228 the AN algorithm yields a damper distribution along the building height which is proportional to the  
 229 distribution corresponding to the optimal design solution, and (2) the optimal design solution lies at the  
 230 boundary of the reliability constraint, i.e., increasing the target failure probability always results in a  
 231 decrease of the dampers cost. It is noteworthy that the results of the application examples presented in this  
 232 study confirm that the second assumption is generally satisfied.

233 The computational cost of the proposed correction is mainly due to the computation of  $P_{f,t_L}^{\text{SIM}}(\mathbf{d}_{AN}^*)$   
 234 through stochastic simulation, whereas the computational cost of evaluating  $\nabla_{\mathbf{d}} P_{f,t_L}^{\text{AN}}(\mathbf{d}_{AN}^*)$  is almost  
 235 negligible. The effects of the MPU on the optimal damper properties can also be included through Eq. (5)  
 236 by using the LHS technique to evaluate  $P_{f,t_L}^{\text{SIM}}(\mathbf{d}_{AN}^*)$ . In general, the proposed first-order correction  
 237 formula provides a start point  $\mathbf{d}_{\text{corr}}^*$  for the SIM and HYB algorithms that is closer to satisfying the  
 238 stochastic constraint on the system failure probability when compared to  $\mathbf{d}_{AN}^*$ , and is often sufficiently  
 239 accurate for design purposes.

240 **Application examples**

241 The reliability-based design methodology and correction formula developed in this study were applied to  
 242 determine the optimal properties and location of viscous dampers under two different design scenarios: (1)  
 243 viscous dampers located inside two adjacent buildings, and (2) viscous dampers connecting two adjacent  
 244 buildings. In the second scenario, the effects of MPU is also considered.

245 The two adjacent buildings considered in this study were steel moment-resisting frames modeled as linear  
 246 elastic multi-degree-of-freedom shear-type systems (Fig. 1). The properties of these buildings, initially  
 247 assumed as deterministic, were taken from Tubaldi et al. (2014). Building A was an eight-story frame with  
 248 constant floor mass,  $m_A = 454,540$  kg, and stiffness,  $k_A = 628,801$  kN/m (Lin 2005). Building B was a four-  
 249 story building with constant floor mass,  $m_B = 454,540$  kg, and stiffness,  $k_B = 470,840$  kN/m. The story  
 250 heights were equal to  $H = 3.2$  m. Matrices  $\mathbf{C}_A$  (with dimensions  $8 \times 8$ ) and  $\mathbf{C}_B$  (with dimensions  $4 \times 4$ )  
 251 describe the inherent buildings' damping. They were based on the Rayleigh model and were obtained by  
 252 assuming a damping factor  $\xi_A = \xi_B = 2\%$  for the first two vibration modes of each system. The fundamental  
 253 vibration periods of buildings A and B were  $T_A = 0.915$  s and  $T_B = 0.562$  s, respectively.

254 The stochastic seismic input considered in this study was modeled as an embedded stationary Gaussian  
 255 process modulated in time through a Shinozuka-Sato's modulating function (Shinozuka and Sato 1967),  
 256 i.e.,

257 
$$I(t) = c \cdot (e^{-b_1 t} - e^{-b_2 t}) \cdot H(t) \quad (6)$$

258 in which  $b_1 = 0.045\pi \text{ s}^{-1}$ ,  $b_2 = 0.050\pi \text{ s}^{-1}$ ,  $c = 25.812$ , and  $H(t)$  = unit step function. A duration  
 259  $t_{\max} = 30$  s was assumed for the seismic excitation. The PSD function of the embedded stationary process  
 260 was described by the widely-used Kanai-Tajimi model, as modified by Clough and Penzien (Clough and  
 261 Penzien 1993), i.e.,

262 
$$S_{CP}(\omega) = S_0 \cdot \frac{\omega_g^4 + 4 \cdot \xi_g^2 \cdot \omega^2 \cdot \omega_g^2}{\left[\omega_g^2 - \omega^2\right]^2 + 4 \cdot \xi_g^2 \cdot \omega^2 \cdot \omega_g^2} \cdot \frac{\omega^4}{\left[\omega_f^2 - \omega^2\right]^2 + 4 \cdot \xi_f^2 \cdot \omega^2 \cdot \omega_f^2} \quad (7)$$

263 in which  $S_0$  = amplitude of the bedrock excitation spectrum, modeled as a white noise process;  $\omega_g$  and  $\xi_g$   
 264 = fundamental circular frequency and damping factor of the soil, respectively; and  $\omega_f$  and  $\xi_f$  =  
 265 parameters describing the Clough-Penzien filter. The following values of the parameters were used:  
 266  $\omega_g = 12.5 \text{ rad/s}$ ,  $\xi_g = 0.6$ ,  $\omega_f = 2 \text{ rad/s}$ , and  $\xi_f = 0.7$ .

267 The peak ground acceleration,  $PGA$ , was assumed as  $IM$ . In order to derive the fragility curves in terms of  
 268 the selected  $IM$ , the relationship between the parameter  $S_0$  of the modified Kanai-Tajimi spectrum and the  
 269  $PGA$  at the site was assessed empirically based on the procedure shown in Tubaldi et al. (2012). The site  
 270 seismic hazard curve was:

$$271 \quad v_{PGA}(pga) = 6.734 \cdot 10^{-5} \cdot pga^{-2.857} \quad (8)$$

272 This seismic hazard curve was chosen so that, for the site of interest, a  $PGA = 0.3 \text{ g}$  (where  $g$  = gravity  
 273 constant) corresponded to a probability of being exceeded equal to 10% in 50 years (i.e., to a return period  
 274 of 475 years).

### 275 ***Design of viscous dampers located inside the buildings***

276 The first application example consists of the design of linear viscous dampers inserted inside the building  
 277 frames. The target performance objective was defined so that the probability  $P_{f,t_L}$  of exceeding the  
 278 immediate occupancy performance level for the coupled system in  $t_L = 50$  years must be less than or equal  
 279 to  $\bar{P}_f = 10\%$ . The component limit states considered corresponded to the exceedance of the interstory drift  
 280 limits of 0.7% by any of the two buildings' stories, as specified in FEMA 273 (1997) and FEMA 356  
 281 (2000). This interstory drift value can be considered as a conventional limit for the linear elastic behavior  
 282 of multi-story steel buildings and for their immediate occupancy limit state, which corresponds to negligible  
 283 structural damage. The assumption of linear elastic behavior was deemed accurate for this specific  
 284 performance level, since the fact that the buildings may experience nonlinear behavior for high (and rare)  
 285  $IM$  values was not expected to bias the risk estimates. The damper limit states were not considered in this  
 286 application, since the dampers are commonly sized so that their failure probability is significantly smaller

287 than the probability of exceedance of the 0.7% drift limit in the frame. It is noteworthy that, in modern  
 288 design codes, the performance objectives are usually expressed as required performance for a seismic event  
 289 with a prescribed return period (FEMA 2000), e.g., as a maximum acceptable drift limit for an earthquake  
 290 intensity with a given probability of being exceeded in 50 years. However, a rigorous reliability-based  
 291 design approach requires selecting the values of the target failure probability for the maximum acceptable  
 292 drift limits at each performance level of interest. Failure probability values and their selection commonly  
 293 depend on the interacting needs of the different stakeholders; thus, the value of 10% failure probability in  
 294 50 years was selected in this study based on engineering judgment and economic considerations.

295 Without dampers, the probabilities of exceedance for the immediate occupancy performance level in 50  
 296 years,  $P_{f,t_L}$ , were 26.07% and 28.55%, for buildings A and B, respectively. Two design options were  
 297 investigated: (1) viscous dampers with uniform properties located at all building stories (referred to as  
 298 uniform distribution case); and (2) viscous dampers with properties variable from story to story (referred  
 299 to as variable distribution case). This latter damper distribution corresponded to eight design variables, i.e.,

300  $\mathbf{d} = [c_{d1}, \dots, c_{d8}]^T$ , for the 8-story building (building A), and to four design variables, i.e.,

301  $\mathbf{d} = [c_{d1}, c_{d2}, c_{d3}, c_{d4}]^T$ , for the 4-story building (building B). The feasible domain for the damper viscous

302 constants was described by the nonlinear constraints  $c_{d,i} \cdot (c_{d,\min} - c_{d,i}) \leq 0$ , where  $c_{d,\min} = 200$  kN·s/m,

303 and by the lower bound  $c_{d,i} \geq 0$ . These constraints ensured that, at any given floor, the optimal solution

304 corresponds either to the case of no dampers or to values of  $c_{d,i} \geq c_{d,\min}$ , which was assumed as the

305 minimum value of the damper viscous constant for which dampers were readily available at a market

306 competitive cost.

307 The AN algorithm employed the modified Vanmarcke's approximation of the time-variant hazard function

308 in conjunction with the assumption of perfect correlation between the failure modes to estimate  $P_{f,t_L}^{AN}(\mathbf{d})$

309 and  $\nabla_{\mathbf{d}} P_{f,t_L}^{AN}(\mathbf{d})$  during the iterations. The estimates of  $P_{f,t_L}^{SIM}(\mathbf{d})$  required at each iteration of the SIM

310 algorithm were obtained via MCS by considering 10,000 artificial ground motion records compatible with

311 the input PSD and generated through the spectral representation method (Shinozuka and Deodatis 1991).  
 312 This number of samples ensured accurate estimates of the MAF of system failure,  $v_f$ , with a coefficient of  
 313 variation of the estimate of  $v_f$  smaller than 1%. The tolerances for the design problem were selected as  
 314  $\varepsilon_1 = \varepsilon_2 = 10^{-3}$ . Multiple start points were considered for the AN algorithm to find the global minimum of  
 315 the objective function. To limit the number of iterations needed for convergence, the AN algorithm's  
 316 optimal solution,  $\mathbf{d}_{AN}^*$ , was used as a hot-start point for the SIM algorithm, the results of which were  
 317 considered as the reference solution for this application example. In applying both AN and SIM algorithms,  
 318 the failure probability's gradients (i.e.,  $\nabla_{\mathbf{d}} P_{f,t_L}^{AN}(\mathbf{d})$  and  $\nabla_{\mathbf{d}} P_{f,t_L}^{SIM}(\mathbf{d})$ , respectively) were computed at each  
 319 iteration using the finite difference method, i.e., by perturbing each component of vector  $\mathbf{d}$  one at a time  
 320 and calculating the corresponding change in failure probability. For this specific application example, the  
 321 use of the modified Vanmarcke's approximation in conjunction with the assumption of perfect correlation  
 322 between failure modes were shown to provide more accurate estimates of the failure probability than other  
 323 analytical approximations (Tubaldi et al. 2014). It is also noteworthy that these approximations can affect  
 324 the value of the optimal solution obtained through the AN algorithm,  $\mathbf{d}_{AN}^*$ , but have only a negligible effect  
 325 on the value of reference optimal solution.

326 Tables 1 and 2 report the optimal design results obtained using the AN algorithm, the correction  
 327 corresponding to Eq. (5), and the SIM algorithm for building A and B, respectively. In all cases considered  
 328 here, the design solution obtained using the AN algorithm is already close to the design solution obtained  
 329 using the SIM algorithm (with a 7.8% difference in the uniform distribution case and a 5.8% difference in  
 330 the variable distribution case for building A, and a -8.3% difference in the uniform distribution case and a  
 331 -7.1% difference in the variable distribution case for building B). The proposed correction formula provides  
 332 dampers' properties that are very close to those obtained through the SIM algorithm (with a 2.8% difference  
 333 in the uniform distribution case and a 0.9% difference in the variable distribution case for building A, and  
 334 a 0.6% difference in the uniform distribution case and a 0.4% difference in the variable distribution case  
 335 for building B). It is observed that the design solution for the variable distribution case requires dampers

336 located only at the two lower stories, and allows to reduce the cost associated with the retrofit (measured  
337 in terms of total added viscous damping) when compared to the design solution corresponding to the  
338 uniform distribution case.

339 Fig. 3a and 3b report the component fragility curves (i.e., failure probabilities conditional to  $PGA$ ) for the  
340 interstory drift ratios (IDRs) and the corresponding failure probabilities during the design life, respectively,  
341 for building A. These estimates correspond to the solution obtained using the SIM algorithm by considering  
342 both the cases of uniform and variable distribution. The curves of the system fragilities and of the system  
343 risk are very close to the corresponding curves for the first story and, thus, they are not reported in Fig. 3a  
344 and 3b. This results is due to the fact that (1) the IDR demand at the first story is higher when compared to  
345 those at the other stories, and (2) the correlation between the IDR responses within the frame is very high.  
346 Figs. 4a and 4b plot the probabilities of exceedance in 50 years for the dampers' forces at the different  
347 stories of building A, corresponding to the uniform and variable distribution cases, respectively. It is  
348 observed that, for a given probability of exceedance, the sum of the dampers' forces in the variable  
349 distribution case is significantly lower than the sum of the dampers' forces in the uniform distribution case.  
350 Thus, the optimal design for the variable distribution case is more efficient than the optimal design for the  
351 uniform distribution case also in terms of the total forces acting in the dampers. Similar results to those  
352 presented in Figs. 3 and 4 were obtained also for building B, but are not reported here due to space  
353 constraints.

#### 354 ***Design of viscous dampers connecting adjacent buildings***

355 The second application example consists of the design of linear viscous dampers connecting two adjacent  
356 buildings with the same properties as the buildings A and B considered in the previous application example.  
357 Two design options were investigated also in this case: (1) viscous dampers with uniform properties  
358 connecting the four lower stories of the two buildings (uniform distribution case), which corresponds to a  
359 single design variable,  $c_d$ ; and (2) viscous dampers with variable properties connecting the four lower  
360 stories of the two buildings (variable distribution case), which corresponds to four design variables,



361  $\mathbf{d} = [c_{d1}, c_{d2}, c_{d3}, c_{d4}]^T$ . Both deterministic and uncertain structural models were investigated. In the latter  
362 case, following Sues et al. (1985), the lumped mass and story stiffness of each building were assumed to  
363 be lognormally distributed, with mean value equal to the value initially assumed as deterministic and  
364 coefficients of variation equal to 0.10 and 0.11, respectively. The damping ratios used to build the Rayleigh  
365 damping matrixes for the two separate systems were also modeled as random variables with mean value  
366 equal to 2% and with coefficient of variation equal to 0.65. Perfect correlation was assumed between the  
367 lumped masses and story stiffness within each building. Thus, six random variables were used to describe  
368 the MPU (i.e., story mass, story stiffness, and damping ratio for each building). Similar to Tubaldi et al.  
369 (2014), the assumption of perfect correlation is preferred here to a more rigorous random field approach  
370 (Lee and Mosalam 2004) in order to avoid difficulties due to the lack of data associated with the correlation  
371 lengths of the pertinent random fields. It is noteworthy that this assumption (which corresponds to assuming  
372 that the correlation length for the corresponding random field is larger than the dimension of the structural  
373 system considered) provides an upper bound of the MPU effects on the failure probability and, thus, on the  
374 reliability-based design results.

375 50 samples of structural models were generated by means of LHS (Iman and Conover 1980), in order to  
376 describe with sufficient accuracy the variability of the uncertain parameters. An exterior sampling approach  
377 was adopted for the study of the uncertain structures, i.e., the same set of 50 LHS realizations of the vector  
378 of uncertain model parameters was employed at each iteration of the SIM algorithm to obtain the  
379 approximate and reference design solutions for the uncertain structural models. The selected sample number  
380 provides estimates of the failure probability at the design points corresponding to structures with uncertain  
381 parameters with coefficient of variations lower than 0.05. The results presented hereinafter correspond to a  
382 single set of parameters' samples. However, in order to assess the effect of using different samples, the  
383 reliability-based design procedure was repeated for several samples' sets and provided design results that  
384 had differences smaller than 0.5% in terms of  $C(\mathbf{d}^*)$ .

385 The probability of exceeding the immediate occupancy performance level in 50 years for the uncoupled

386 deterministic system was estimated equal to 33.8% by using MCS. The same constraints, target  
387 performance objectives, and termination rules employed in the previous application example were adopted  
388 also here. The AN algorithm was based on the modified Vanmarcke's approximation and the assumption  
389 of perfect correlation between the failure modes. The failure probability estimates used in the SIM  
390 algorithm were obtained using MCS and 10,000 samples. Multiple start points were considered for the AN  
391 algorithm to find the global minimum of the objective function, and the design point obtained from the AN  
392 algorithm was used as a hot-start point for the SIM algorithm.

393 Tables 3 and 4 report the optimal design results obtained using the AN algorithm, the proposed correction  
394 formula, and the SIM algorithm for the deterministic and uncertain models, respectively. When compared  
395 to the design solution obtained using the SIM algorithm, the design solution obtained using the AN  
396 algorithm is a fair approximation for the case of deterministic models (with a 22.0% difference in the  
397 uniform distribution case and a 24.4% difference in the variable distribution case) and a very good  
398 approximation for the case of uncertain models (with a 0.8% difference in the uniform distribution case and  
399 a 2.2% difference in the variable distribution case). The proposed correction formula provides dampers'  
400 properties that are always an excellent approximation of those obtained through the SIM algorithm (with a  
401 0.8% difference in the uniform distribution case and a 2.0% difference in the variable distribution case for  
402 the deterministic models, and a 0.8% difference in the uniform distribution case and a 0.3% difference in  
403 the variable distribution case for the uncertain models).

404 It is observed that, in general, the uncertainty in model parameters results in an increase of the total added  
405 damping,  $C(\mathbf{d}^*)$ , at the optimal design point,  $\mathbf{d}^*$ , due to an increase of the seismic risk (Tubaldi et al.  
406 2014). For both deterministic and uncertain models, the value of  $C(\mathbf{d}^*)$  is significantly lower for the  
407 variable distribution case than for the uniform distribution case. Similar observations were already made in  
408 previous studies (Zhang and Xu 1999, Roh et al. 2011) and can be explained by considering that the energy  
409 dissipated by the damper(s) is roughly proportional to the maximum relative velocity between the stories  
410 of the two buildings. Since this relative velocity generally increases for increasing heights of the damper

411 location, it is more efficient to locate the dampers at the upper stories of the buildings, where the peak  
412 relative velocity is expected to be the highest. At the optimal design points, the first-mode damping ratios  
413 of the deterministic models of buildings A and B are 0.160 and 0.063, respectively, for the uniform  
414 distribution case, and 0.155 and 0.068, respectively, for the variable distribution case.

415 Fig. 5 plots the probability of exceedance in 50 years (evaluated using the SIM algorithm) for the IDRs of  
416 the first story of building A and B for the two different optimal dampers' distributions. Fig. 5a shows the  
417 results for the case of deterministic model parameters, whereas Fig. 5b shows the results for the case of  
418 uncertain model parameters. In both cases, it is observed that the distribution of the peak interstory drift  
419 demand at the various stories is not significantly affected by the dampers' configuration. This result  
420 confirms that employing only a single damper at the optimal location permits to achieve the same system  
421 performance of four uniformly distributed dampers at a significantly lower value of the total added  
422 damping.

423 The statistical properties of the strokes and forces produced in the dampers are also relevant design  
424 quantities that can affect the dampers' reliability and actual cost (Hwang et al. 2013). Fig. 6a reports the  
425 50-year probability of exceeding a specified value of the stroke in the dampers for the optimal designs  
426 corresponding to the uniform and variable distribution cases, relative to the deterministic model case. As  
427 expected, in the uniform distribution case, the strokes corresponding to a given probability of exceedance  
428 increase at the upper floors. Furthermore, the single damper corresponding to the variable distribution case  
429 (which is located at the fourth floor) shows probabilities of exceeding a given stroke that are almost  
430 coincident to those of the damper located at the fourth floor in the uniform distribution option. Fig. 6b  
431 reports the 50-year probability of exceeding a specified value of the force acting in each individual damper  
432 and the sum of the forces acting in all dampers, for the optimal designs corresponding to the uniform and  
433 variable distribution cases, relative to the deterministic model case. For a given probability of exceedance,  
434 the force acting in the single damper corresponding to the optimal design for the variable distribution case  
435 is significantly higher than the forces acting in each of the dampers for the uniform distribution case. This  
436 phenomenon is expected because the design requiring the smallest number of dampers is also characterized

437 by the largest damper force (Hwang et al. 2013). However, for the same probability of exceedance, the sum  
438 of the forces acting in all dampers for the uniform distribution case is significantly higher than the force  
439 acting in the single damper for the variable distribution case. Thus, the optimal design for the variable  
440 distribution case is more efficient than the optimal design for the uniform distribution case also with respect  
441 to the values of the forces acting in the dampers.

## 442 **Conclusions**

443 This study presents a reliability-based methodology for the seismic design of linear viscous/visco-elastic  
444 damping devices within and/or between adjacent buildings structures. The proposed methodology, which  
445 is consistent with modern performance-based earthquake engineering frameworks, considers the  
446 uncertainty affecting both the seismic input (i.e., record-to-record variability and uncertain intensity level)  
447 and the model parameters. The optimal design of the dampers' properties and location for a target  
448 performance objective is cast in the form a constrained optimization problem with a deterministic objective  
449 function (e.g., dampers' cost) and a stochastic constraint on the system failure probability during the  
450 buildings' design life.

451 The general approach proposed in this study was specialized to the case of buildings with linear elastic  
452 behavior under non-stationary stochastic earthquake input, in order to take advantage of an efficient  
453 analytical technique to evaluate the system failure probability during the optimization process. The AN  
454 algorithm, previously developed by the authors to obtain the optimal separation distance to avoid seismic  
455 pounding between two adjacent buildings, was extended here to obtain an approximate solution of the  
456 optimal design of the of the dampers' properties and location. A correction formula for the solution provided  
457 by the AN algorithm was proposed to obtain an improved design solution at a small computational cost.

458 The proposed design methodology was illustrated by considering the retrofit of two steel buildings, modeled  
459 as shear-type multi-degree-of-freedom linear elastic systems, by using viscous dampers. The application  
460 examples considered include individual and coupled buildings, deterministic and uncertain structural  
461 models, and viscous dampers characterized by uniform and variable properties at the various buildings'  
462 stories. The dampers' viscous constants were assumed as design variables. Their optimal values were

463 obtained by minimizing the total added damping while satisfying the stochastic constraints on the  
464 probability of exceeding the immediate occupancy level during the buildings' design life. Based on the  
465 results obtained using the proposed design methodology for the application examples presented in this  
466 paper, the following observations are made:

467 (1) The AN algorithm is very computationally efficient but does not strictly satisfy the stochastic constraint  
468 on the system probability of exceeding the target performance level.

469 (2) In general, the proposed correction formula provides approximate solutions that are very close to the  
470 optimal design obtained using SIM and HYB algorithms at a very small computational cost in addition to  
471 the computational cost of the AN algorithm. This computational cost is several orders of magnitude smaller  
472 than the computational cost required by the SIM and HYB algorithms, even when the solution obtained  
473 from the AN algorithm is used as a hot-start point.

474 (3) Model parameter uncertainty commonly produces an increase of the seismic risk estimates, which  
475 causes an increase of the total added damping for the uncertain model case when compared to the case of  
476 deterministic model.

477 (4) For the application examples considered here, optimization of the damper location yields a significant  
478 reduction of the total added damping required to achieve a target performance level when compared to a  
479 design option in which equal dampers are used at different stories within a building or between adjacent  
480 buildings.

481 (5) The design methodology presented in this study provides a simple yet efficient technique for the optimal  
482 design and placement of viscous/visco-elastic dissipative devices into linear elastic structural systems while  
483 controlling their seismic performance.

#### 484 **Acknowledgements**

485 The authors gratefully acknowledge support of this research by (1) the Louisiana Board of Regents (LA  
486 BoR) through the Pilot Funding for New Research (Pfund) Program of the National Science Foundation  
487 (NSF) Experimental Program to Stimulate Competitive Research (EPSCoR) under Award No.  
488 LEQSF(2013)-PFUND-305; (2) the LA BoR through the Louisiana Board of Regents Research and

489 Development Program, Research Competitiveness (RCS) subprogram, under Award No. LESQSF(2010-  
490 13)-RD-A-01; and (3) the LA Department of Wildlife and Fisheries through award #724534. Any opinions,  
491 findings, conclusions or recommendations expressed in this publication are those of the authors and do not  
492 necessarily reflect the views of the sponsors.

## 493 **References**

494 Au, S.K., Beck, J.L. (2001a). "First excursion probabilities for linear systems by very efficient importance  
495 sampling." *Prob. Eng. Mech.*, 16(3), 193-207.

496 Au, S.K., Beck, J.L. (2001b). "Estimation of small failure probabilities in high dimensions by subset  
497 simulation." *Prob. Eng. Mech.*, 16(4), 263-277.

498 Barbato, M., Conte, J.P. (2008). "Spectral characteristics of non-stationary random processes: Theory and  
499 applications to linear structural models." *Prob. Eng. Mech.*, 23(4), 416-426.

500 Barbato, M., Vasta, M. (2010). "Closed-form solutions for the time-variant spectral characteristics of non-  
501 stationary random processes." *Prob. Eng. Mech.*, 25(1), 9-17.

502 Barbato, M., Conte, J.P., (2011). "Structural Reliability Applications of Nonstationary Spectral  
503 Characteristics." *J. Eng. Mech.*, 137(5), 371-382.

504 Barbato, M., Tubaldi, E. (2013). "A probabilistic performance-based approach for mitigating the seismic  
505 pounding risk between adjacent buildings." *Earthquake Eng. Struct. Dyn.*, 42(8): 1203-1219.

506 Barbato, M., Conte, J. (2014). "Time-Variant Reliability Analysis of Linear Elastic Systems Subjected to  
507 Fully Nonstationary Stochastic Excitations." *J. Eng. Mech.*, [10.1061/\(ASCE\)EM.1943-7889.0000895](https://doi.org/10.1061/(ASCE)EM.1943-7889.0000895) ,  
508 04014173.

509 Bhaskararao, A.V., Jangid, R.S. (2007). "Optimum viscous damper for connecting adjacent SDOF  
510 structures for harmonic and stationary white-noise random excitations." *Earthquake Eng. Struct. Dyn.*,  
511 36(4), 563-571.

512 Clough, R.W., Penzien, J. (1993). *Dynamics of Structures*, Mc.Graw Hill: New York, US.

513 Federal Emergency Management Agency (FEMA) (1997). *NEHRP Guidelines for the Seismic  
514 Rehabilitation of Buildings*, FEMA Publication 273, Washington D.C., US.

515 Federal Emergency Management Agency (FEMA) (2000). *Prestandard and Commentary for the Seismic*  
516 *Rehabilitation of Buildings*, FEMA Publication 356, Washington D.C., US.

517 Guo, A.X., Xu, Y.L., Wu, B. (2002). "Seismic reliability analysis of hysteretic structure with viscoelastic  
518 dampers." *Eng. Struct.*, 24(3), 373-383.

519 Hwang, J.S., Lin, W.C., Wu, N.J. (2013). "Comparison of distribution methods for viscous damping  
520 coefficients to buildings." *Struct. and Infrastr. Eng.*, 9(1), 28-41.

521 Iman, R.L., Conover, W. (1980). "Small sample sensitivity analysis techniques for computer models, with  
522 an application to risk assessment." *Communication in Statistics*, 9(17):1749-1842.

523 Jensen, H.A., Valdebenito, M.A., Schuëller, G.I., Kusanovic, D.S. (2009). "Reliability-based optimization  
524 of stochastic systems using line search." *Comp. Methods in Appl. Mech. and Eng.*, 198(49-52), 3915-3924.

525 Jensen, H.A., Sepulveda, J.G. (2011). "Structural optimization of uncertain dynamical systems considering  
526 mixed-design variables." *Prob. Eng. Mech.*, 26(2), 269-280.

527 Jensen, H.A., Sepulveda, J.G. (2012). "On the reliability-based design of structures including passive  
528 energy dissipation systems." *Struct. Saf.*, 34(1), 390-400.

529 Lin, J.H. (2005). "Evaluation of seismic pounding risk of buildings in Taiwan." *Chin Inst Eng*, 28:867-72.

530 Kim, K., Rye, J., Chung, L. (2006). "Seismic performance of structures connected by viscoelastic dampers."  
531 *Eng. Struct.*, 28(2), 183-195.

532 Lee, T.H., Mosalam, K.M. (2004). "Probabilistic fibre element modeling of reinforced concrete structures."  
533 *Comp. and Struct.*, 82(27), 2285-2299.

534 Lin, J.H. (2005). "Evaluation of seismic pounding risk of buildings in Taiwan." *Chin Inst Eng*, 28:867-72.

535 Luco, N., Cornell, C.A. (2007). "Structure-specific scalar intensity measures for near-source and ordinary  
536 earthquake ground motions." *Earth. Spect.*, 23(2), 357-392.

537 Marano, C., Trentadue, F., Greco, R. (2007). "Stochastic Optimum design criterion for linear damper  
538 devices for seismic protection of buildings." *Struct. and Mult. Optim.*, 33(6), 441-455.

539 MathWorks, Inc. (2015). *Matlab R2015a - Global Optimization Toolbox Documentation*,  
540 <http://www.mathworks.com/help/gads/global-or-multiple-starting-point-search.html> accessed online on  
541 April 8, 2015.

542 Park, K.S., Koh, H.M., Hahm, D. (2004). "Integrated optimum design of viscoelastically damped structural  
543 systems." *Eng. Struct.*, 26(5), 581-591.

544 Richardson, A., Walsh, K.K., Abdullah, M.M. (2012). "Closed-form equations for coupling linear  
545 structures using stiffness and damping elements." *Struct. Contr. and Health Monit.*, 20(3), 259-281.

546 Roh, H., Cimellaro, G.P., Lopez-Garcia, D. (2011). "Seismic Response of Adjacent Steel Structures  
547 Connected by Passive Device." *Adv. in Struct. Eng.*, 14(3), 499-517.

548 Shinozuka, M., Sato, Y. (1967). "Simulation of nonstationary random processes.", *J. of Eng. Mech.*  
549 *Division*, 93(EM1), 11-40.

550 Shinozuka, M, Deodatis, G. (1991). "Simulation of stochastic processes by spectral representation." *Appl.*  
551 *Mech. Rev.*, 44(4), 191-203.

552 Soong, T.T., Spencer, B.F. (2002). "Supplemental energy dissipation: state-of-the-art and state-of-the-  
553 practice." *Eng. Struct.*, 24(3), 243-259.

554 Shukla, A. and Datta, T. (1999). "Optimal Use of Viscoelastic Dampers in Building Frames for Seismic  
555 Force." *J. Struct. Eng.*, 125(4), 401-409.

556 Sues, R.H., Wen, Y.K., Ang, AH-S. (1985). "Stochastic evaluation of seismic structural performance."  
557 *ASCE Journal of Structural Engineering*, 111(6), 1204-1218.

558 Taflanidis, A.A., Beck, J.L. (2008). "An efficient framework for optimal robust stochastic system design  
559 using stochastic simulation." *Comp. Methods in Appl. Mech. and Eng.*, 198(1), 88-101.

560 Taflanidis, A.A. (2010). "Reliability-based optimal design of linear dynamical systems under stochastic  
561 stationary excitation and model uncertainty." *Eng. Struct.*, 32(5), 1446-1458.

562 Taflanidis, A., Scruggs, J. (2010). "Performance measures and optimal design of linear structural systems  
563 under stochastic stationary excitation." *Struct. Saf.*, 32(5), 305-315.



564 Takewaki, I. (2009). Building control with passive dampers: Optimal performance-based design for  
565 earthquakes. Singapore: John Wiley & Sons (Asia).

566 Tubaldi, E., Barbato, M., Dall'Asta, A. (2014). "Performance-based seismic risk assessment for buildings  
567 equipped with linear and nonlinear viscous dampers." *Eng. Struct.*, 78, 90-99.

568 Tubaldi, E., Barbato, M., Ghazizadeh, S. (2012). "A probabilistic performance-based risk assessment  
569 approach for seismic pounding with efficient application to linear systems." *Struct. Saf.*, 36-37, 14-22.

570 Tubaldi, E. (2015). "Dynamic behavior of adjacent buildings connected by linear viscous/viscoelastic  
571 dampers." *Struct. Contr. and Health Monit.*. DOI: 10.1002/stc.1734.

572 Ugray, Z., Lasdon, L., Plummer, J.C., Glover, F., Kelly, J., Martí R. (2007). "Scatter Search and Local NLP  
573 Solvers: A Multistart Framework for Global Optimization." *INFORMS J. on Comp.*, 19(3), 328-340.

574 Zhang, W.S., Xu, Y.L. (1999). "Dynamic characteristics and seismic response of adjacent buildings linked  
575 by discrete dampers." *Earthquake Eng. Struct. Dyn.*, 28(10), 1163-1185.

576 Zhu, H.P., Ge, D.D., Huang, X. (2011). "Optimum connecting dampers to reduce the seismic responses of  
577 parallel structures." *J. of Sound and Vibr.*, 330(9), 1931-1949.

578

579

Table 1. Optimal design of viscous dampers placed inside building A.

Story number	Uniform distribution			Variable distribution		
	$\mathbf{d}_{AN}^*$ [kN·s/m]	$\mathbf{d}_{corr}^*$ [kN·s/m]	$\mathbf{d}_{SIM}^*$ [kN·s/m]	$\mathbf{d}_{AN}^*$ [kN·s/m]	$\mathbf{d}_{corr}^*$ [kN·s/m]	$\mathbf{d}_{SIM}^*$ [kN·s/m]
1	5,826.70	5,561.90	5,407.48	18,376.80	17,538.45	17,718.94
2	5,826.70	5,561.90	5,407.48	5,726.50	5,465.26	5,068.33
3	5,826.70	5,561.90	5,407.48	0	0	0
4	5,826.70	5,561.90	5,407.48	0	0	0
5	5,826.70	5,561.90	5,407.48	0	0	0
6	5,826.70	5,561.90	5,407.48	0	0	0
7	5,826.70	5,561.90	5,407.48	0	0	0
8	5,826.70	5,561.90	5,407.48	0	0	0
Sum	46,613.60	44,495.20	43,259.84	24,103.30	23,003.71	22,787.28
$P_{f,TL}$	9.65%	9.92%	10.05%	9.71%	9.95%	10.00%

580

581

582

Table 2. Optimal design of viscous dampers placed inside building B.

Story number	Uniform distribution			Variable distribution		
	$\mathbf{d}_{AN}^*$ [kN·s/m]	$\mathbf{d}_{corr}^*$ [kN·s/m]	$\mathbf{d}_{SIM}^*$ [kN·s/m]	$\mathbf{d}_{AN}^*$ [kN·s/m]	$\mathbf{d}_{corr}^*$ [kN·s/m]	$\mathbf{d}_{SIM}^*$ [kN·s/m]
1	2,631.50	2,886.91	2,869.38	6,041.30	6,524.60	6,500.90
2	2,631.50	2,886.91	2,869.38	0	0	0
3	2,631.50	2,886.91	2,869.38	0	0	0
4	2,631.50	2,886.91	2,869.38	0	0	0
Sum	10,526.00	11,547.65	11,477.52	6,041.30	6,524.60	6,500.90
$P_{f,t_L}$	10.71%	9.98%	10.07%	10.81%	10.10%	9.95%

583

584

585  
586

Table 3. Optimum design properties of viscous dampers connecting buildings A and B: deterministic models.

Story number	Uniform distribution			Variable distribution		
	$\mathbf{d}_{AN}^*$ [kN·s/m]	$\mathbf{d}_{corr}^*$ [kN·s/m]	$\mathbf{d}_{SIM}^*$ [kN·s/m]	$\mathbf{d}_{AN}^*$ [kN·s/m]	$\mathbf{d}_{corr}^*$ [kN·s/m]	$\mathbf{d}_{SIM}^*$ [kN·s/m]
1	1,363.51	1,126.40	1,117.63	0	0	0
2	1,363.51	1,126.40	1,117.63	0	0	0
3	1,363.51	1,126.40	1,117.63	0	0	0
4	1,363.51	1,126.40	1,117.63	3,044.85	2,496.49	2,447.51
Sum	5,454.04	4,505.6	4,470.52	3,044.85	2,496.49	2,447.51
$P_{f,t_L}$	8.92%	9.98%	10.00%	8.97%	9.98%	10.00%

587  
588

589  
590

Table 4. Optimum design properties of viscous dampers connecting buildings A and B:  
uncertain models.

Story number	Uniform distribution			Variable distribution		
	$\mathbf{d}_{AN}^*$ [kN·s/m]	$\mathbf{d}_{corr}^*$ [kN·s/m]	$\mathbf{d}_{SIM}^*$ [kN·s/m]	$\mathbf{d}_{AN}^*$ [kN·s/m]	$\mathbf{d}_{corr}^*$ [kN·s/m]	$\mathbf{d}_{SIM}^*$ [kN·s/m]
1	1,363.51	1,363.51	1,353.14	0	0	0
2	1,363.51	1,363.51	1,353.14	0	0	0
3	1,363.51	1,363.51	1,353.14	0	0	0
4	1,363.51	1,363.51	1,353.14	3,044.85	2,987.68	2,979.21
Sum	5,454.04	5,454.04	5,412.56	3,044.85	2,987.68	2,979.21
$P_{f,t_L}$	9.98%	9.98%	10.00%	9.98%	9.99%	10.02%

591

592 **Figure captions**

593 Fig. 1. Buildings equipped with visco-elastic dampers placed inside and between the buildings.

594 Fig. 2. Graphical representation of the correction formula.

595 Fig. 3. Failure probabilities for building A: (a) component fragility curves, and (b) component failure  
596 probabilities during the design life.

597 Fig. 4. Probability of dampers' forces exceeding prescribed values in 50 years in building A: (a) uniform  
598 distribution case, and (b) variable distribution case.

599 Fig. 5. Probability of exceedance in 50 years for the IDRs of the models with (a) deterministic properties,  
600 and (b) uncertain properties.

601 Fig. 6. Probability of exceeding in 50 years for the deterministic models of: (a) dampers' strokes, and  
602 (b) dampers' forces.

Figure 1

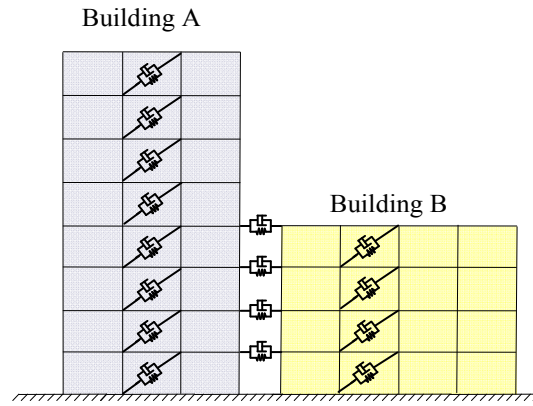


Figure 2

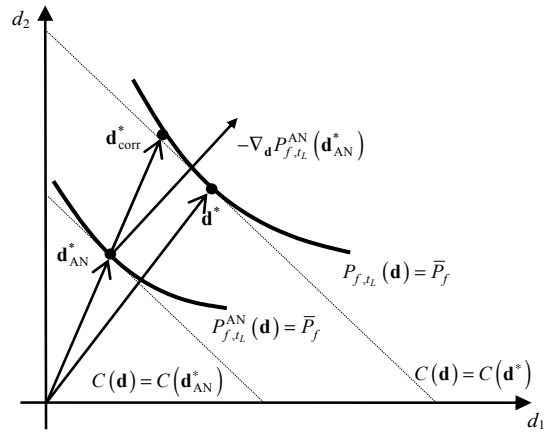




Figure 3

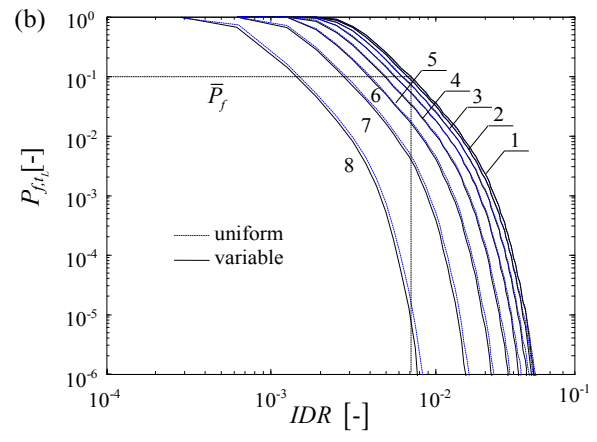
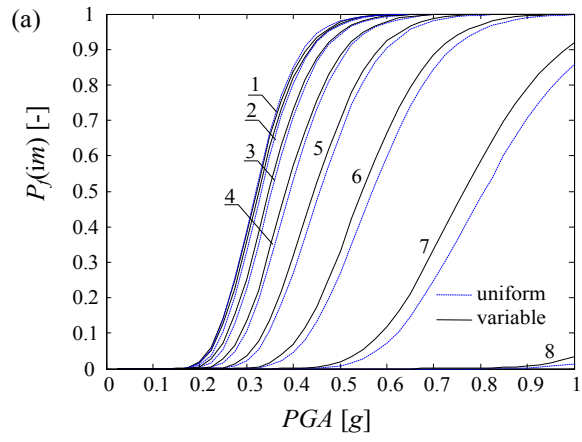


Figure 4

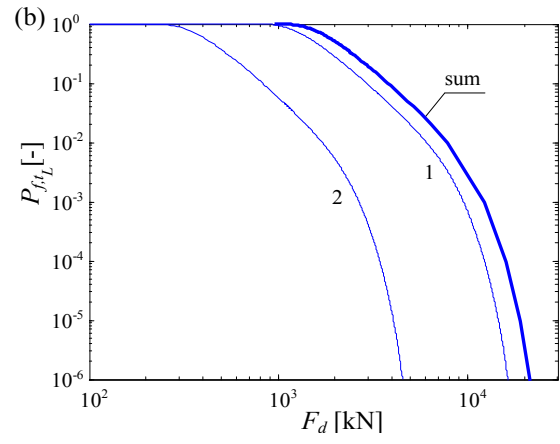
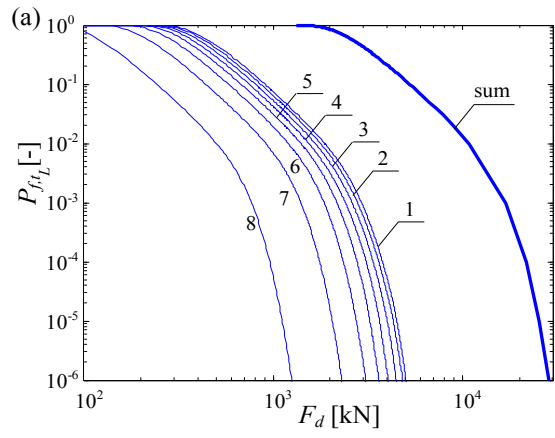


Figure 5

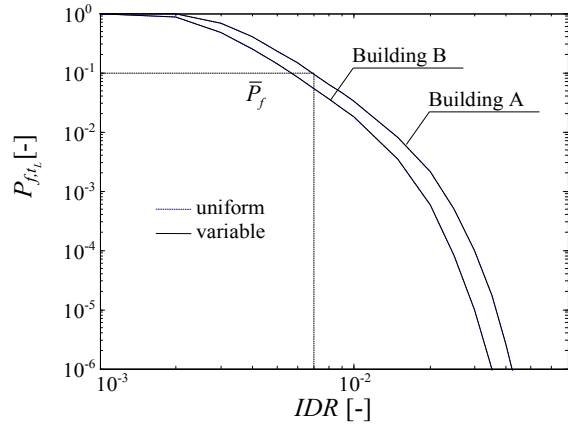
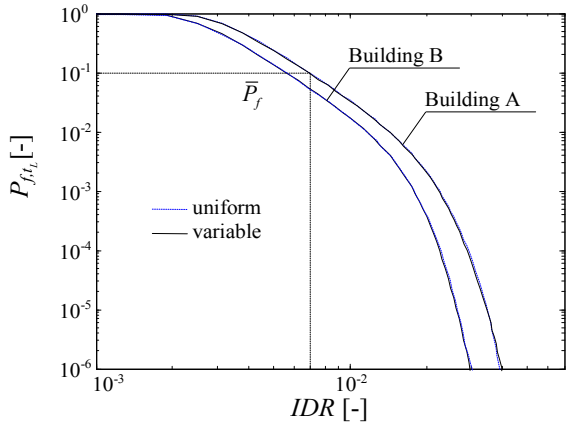


Figure 6

